Chapter 17
Vibrating Particles System Algorithm

17.1 Introduction

In the recent years, many metaheuristics with different philosophies and characteristics are introduced and applied to a wide range of fields. The aim of these optimization methods is to efficiently explore the search space in order to find global or near-global solutions. Since they are not problem specific and do not require the derivatives of the objective function, they have received increasing attention from both academia and industry.

A novel population-based metaheuristic algorithm based on the damped free vibration of single degree of freedom system is introduced in Kaveh and Ilchi Ghazaan [1]. This algorithm is called a vibrating particles system (VPS) algorithm and considers each candidate solution as a particle that approaches its equilibrium position. By utilizing a combination of randomness and exploitation of obtained results, the quality of the particles improves iteratively as the optimization process proceeds. Here, viability of the proposed method is examined using the optimal design of two truss and two frame structures. The selected examples are among the most popular benchmarks previously studied by the researchers (Saka [2], Erbatur et al. [3], Lee and Geem [4], Hasançebi et al. [5], and Kazemzadeh Azad and Hasançebi [6]). The numerical results indicate the efficiency of the proposed algorithm compared to some other methods available in the literature.

The remaining sections of this chapter are organized as follows: The mathematical formulations of the structural optimization are presented in Sect. 17.2. The physical background of the VPS algorithm is presented in Sect. 17.3, and Sect. 17.4 introduces this new optimization method in detail. Section 17.5 investigates the parameter settings and the search behavior of the proposed method, and four structural design examples are studied in Sect. 17.6. Finally, concluding remarks are provided in Sect. 17.7.

A. Kaveh, *Advances in Metaheuristic Algorithms for Optimal Design of Structures*,
DOI 10.1007/978-3-319-46173-1_17

17.2 Formulation of the Structural Optimization Problems

In this study, the objective is to minimize the weight of the structure while satisfying some constraints on stresses and/or buckling and/or deflection and/or natural frequencies. The design variables are cross-sectional areas of structural elements. The mathematical formulation of these problems is expressed as follows:

$$\begin{aligned} &\text{Find} && \{X\} = \left[x_1, x_2, .., x_{ng}\right] \\ &\text{to minimize} && W(\{X\}) = \sum_{i=1}^{nm} \rho_i A_i L_i \\ &\text{subjected to :} && \begin{cases} g_j(\{X\}) \le 0,\ j = 1, 2, \ldots, nc \\ \mathrm{x_{i\ min}} \le x_{\mathrm{i}} \le x_{i\max} \end{cases} \end{aligned} \tag{17.1}$$

where $\{X\}$ is a vector containing the design variables; ng is the number of design variables; $W(\{X\})$ is the weight of the structure; nm is the number of elements of the structure; ρ_i, A_i, and L_i denote the material density, cross-sectional area, and the length of the ith member, respectively; x_{imin} and x_{imax} are the lower and upper bounds of the design variable x_i, respectively; $g_j(\{X\})$ denotes design constraints; and nc is the number of constraints.

To handle the constraints, the well-known penalty approach is employed. Thus, the objective function is redefined as follows:

$$f(\{X\}) = (1 + \varepsilon_1.\upsilon)^{\varepsilon_2} \times W(\{X\}), \qquad \upsilon = \sum_{j=1}^{nc} \max\left[0, g_j(\{X\})\right] \tag{17.2}$$

where υ denotes the sum of the violations of the design constraints. The constant ε_1 is set equal to 1 while ε_2 starts from 1.5 and linearly increases to 3. Such a scheme penalizes the unfeasible solutions more severely as the optimization process proceeds. As a result, in the early stages, the agents are free to explore the search space, but at the end they tend to choose solutions with no violation.

17.3 The Damped Free Vibration

A vibration is the oscillating motion of a particle or a body about a position of equilibrium. In general, there are two types of vibrations: (1) free vibration and (2) forced vibration. When the motion is maintained by the restoring forces only, the vibration is said to be a free vibration, and when a time-dependent force is applied to the system, the resulting motion is described as a forced vibration. In the study of a vibrating system, the effects of friction can be neglected resulting in an undamped vibration. However, all vibrations are actually damped to some degree by friction forces. These forces can be caused by dry friction, or Coulomb friction, between rigid bodies, by fluid friction when a rigid body moves in a fluid, or by

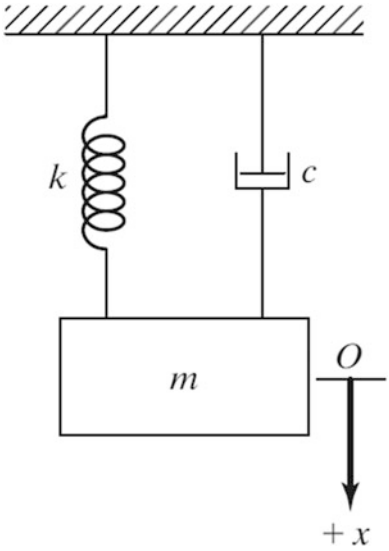

Fig. 17.1 Free vibration of a system with damping

internal friction between the molecules of a seemingly elastic body. In this section, the free vibration of single degree of freedom systems with viscous damping is studied. The viscous damping is caused by fluid friction at low and moderate speeds. Viscous damping is characterized by the fact that the friction force is directly proportional and opposite to the velocity of the moving body (Beer et al. [7]).

The vibrating motion of a body or system of mass m having viscous damping can be characterized by a block and a spring of constant k that is shown in Fig. 17.1. The effect of damping is provided by the dashpot connected to the block, and the magnitude of the friction force exerted on the plunger by the surrounding fluid is equal to $c\dot{x}$ (c is the coefficient of viscous damping, and its value depends on the physical properties of the fluid and the construction of the dashpot). If the block is displaced a distance x from its equilibrium position, the equation of motion can be expressed as:

$$m\ddot{x} + c\dot{x} + kx = 0 \tag{17.3}$$

Before presenting the solutions for this differential equation, we define the critical damping coefficient c_c as:

$$c_c = 2m\omega_n \tag{17.4}$$

$$\omega_n = \sqrt{\frac{k}{m}} \tag{17.5}$$

where ω_n is the natural circular frequency of the vibration.

Depending on the value of the coefficient of viscous damping, three different cases of damping can be distinguished: (1) over-damped system ($c > c_c$), (2) critically

damped system ($c = c_c$), and (3) under-damped system ($c < c_c$). The solutions of over-damped and critically damped systems correspond to a nonvibratory motion. Therefore, the system only oscillates and returns to its equilibrium position when $c < c_c$.

The solution of Eq. (17.3) for under-damped system is as follows:

$$x(t) = \rho e^{-\xi\omega_n t} \sin(\omega_D t + \varphi) \tag{17.6}$$

$$\omega_D = \omega_n \sqrt{1 - \xi^2} \tag{17.7}$$

$$\xi = \frac{c}{2m\omega_n} \tag{17.8}$$

where ρ and φ are constants generally determined from the initial conditions of the problem and ω_D and ξ are damped natural frequency and damping ratio, respectively. Equation (17.6) is shown in Fig. 17.2, and the effect of damping ratio on vibratory motion is illustrated in Fig. 17.3.

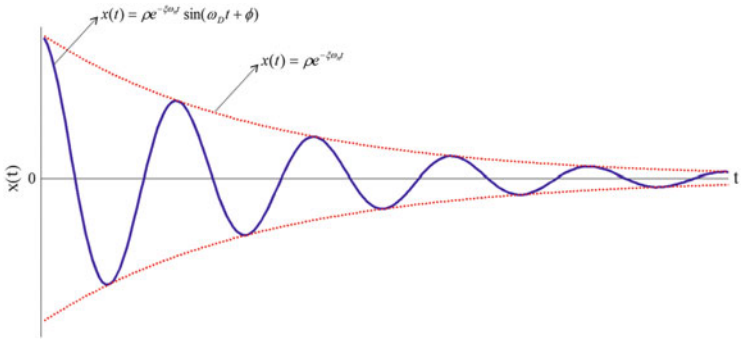

Fig. 17.2 Vibrating motion of under-damped system

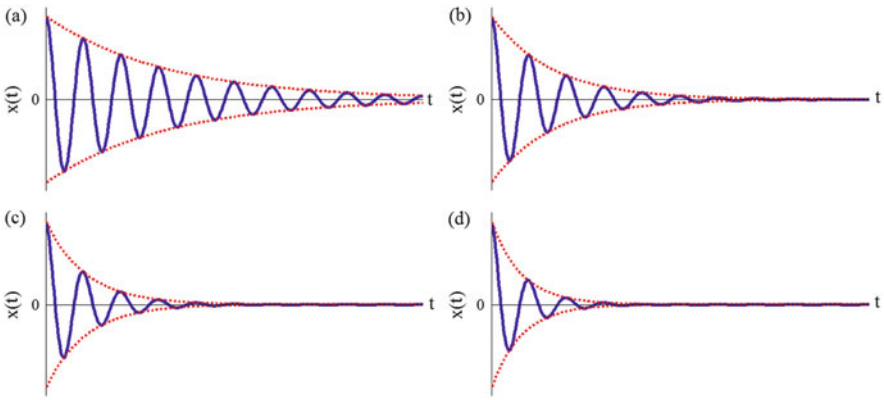

Fig. 17.3 Free vibration of systems with four levels of damping: (**a**) $\xi = 5\%$, (**b**) $\xi = 10\%$, (**c**) $\xi = 15\%$, and (**d**) $\xi = 20\%$

17.4 A New Metaheuristic Algorithm Based on the Vibrating Particles System

The vibrating particles system is a metaheuristic method inspired by the free vibration of single degree of freedom systems with viscous damping. The VPS involves a number of candidate solutions which represent the particles system. The particles are initialized randomly in an n-dimensional search space and gradually approach to their equilibrium positions. The pseudo code of VPS is provided in Fig. 17.4.

The steps of the VPS are as follows:

Step 1: Initialization
The VPS parameters are set and the initial positions of all particles are determined randomly in an n-dimensional search space.

Step 2: Evaluation of Candidate Solutions
The objective function value is calculated for each particle.

Step 3: Updating the Particle Positions
For each particle, three equilibrium positions with different weights are defined that the particle tends to approach: (1) the best position achieved so far across the entire population (*HB*), (2) a good particle (*GP*), and (3) a bad particle (*BP*). In order to select the *GP* and *BP* for each candidate solution, the current population is sorted according to their objective function values in an increasing order, and then *GP* and *BP* are chosen randomly from the first and second half, respectively.

Figure 17.3 shows the important effect of damping level in the vibration. In order to model this phenomenon in the optimization algorithm, a descending function that is a function of the number of iterations is proposed as follows:

```
procedure Vibrating Particles System (VPS)
    Initialize algorithm parameters
    Initial positions are created randomly
    The values of objective function are evaluated and HB is stored
    While maximum iterations is not fulfilled
        for each particle
            The GP and BP are chosen
            if P<rand
                w3=0 and w2=1-w1
            end if
            for each component
                New location is obtained by Eq. (17.10)
            end for
            Violated components are regenerated by harmony search-based handling approach
        end for
        The values of objective function are evaluated and HB is updated
    end while
end procedure
```

Fig. 17.4 Pseudo code of the vibrating particles system algorithm

$$D = \left(\frac{iter}{iter_{\max}}\right)^{-\alpha} \tag{17.9}$$

where *iter* is the current iteration number and $iter_{max}$ is the total number of iterations for optimization process. α is a constant, and Fig. 17.5 shows the effect of this parameter on D.

According to the mentioned concepts, the positions are updated by:

$$x_i^j = w_1.\left[D.A.rand1 + HB^j\right] + w_2.\left[D.A.rand2 + GP^j\right] + w_3.\left[D.A.rand3 + BP^j\right] \tag{17.10}$$

$$A = \left[w_1.\left(HB^j - x_i^j\right)\right] + \left[w_2.\left(GP^j - x_i^j\right)\right] + \left[w_3.\left(BP^j - x_i^j\right)\right] \tag{17.11}$$

$$w_1 + w_2 + w_3 = 1 \tag{17.12}$$

where x_i^j is the jth variable of particle i; w_1, w_2, and w_3 are three parameters to measure the relative importance of *HB*, *GP*, and *BP*, respectively; and *rand*1, *rand*2, and *rand*3 are random numbers uniformly distributed in the range of [0, 1]. The effects of the parameters A and D in Eq. (17.10) are similar to those of ρ and $e^{-\xi\omega_n t}$ in Eq. (17.6), respectively. Also, the value of $\sin(\omega_D t + \varphi)$ is considered unity in Eq. (17.10) ($x(t) = \rho e^{-\xi\omega_n t}$ is shown in Fig. 17.2 by red lines).

A parameter like p within (0, 1) is defined, which specifies whether the effect of *BP* must be considered in updating position or not. For each particle, p is compared with *rand* (a random number uniformly distributed in the range of [0, 1]) and if $p <$ rand, then $w_3 = 0$ and $w_2 = 1 - w_1$.

Three essential concepts consisting of self-adaptation, cooperation, and competition are considered in this algorithm. Particles move toward *HB* so the

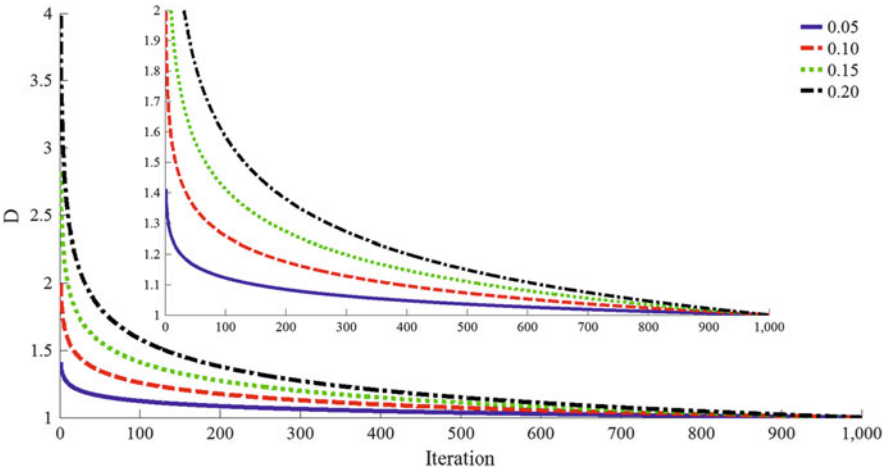

Fig. 17.5 The influence of α on D function

self-adaptation is provided. Any particle has the chance to have influence on the new position of the other one, so the cooperation between the particles is supplied. Because of the p parameter, the influence of GP (good particle) is more than that of BP (bad particle), and therefore the competition is provided.

Step 4: Handling the Side Constraints
The particle moves in the search space to find a better result and it may violate the side constraints. If any component of the system violates a boundary, it must be regenerated by harmony search-based side constraint handling approach (Kaveh and Talatahari [8]). In this technique, there is a possibility like *HMCR* (harmony memory considering rate) that specifies whether the violating component should be regenerated considering the corresponding component of the historically best position of a random particle or it should be determined randomly in the search space. Moreover, if the component of a historically best position is selected, there is a possibility like *PAR* (pitch adjusting rate) that specifies whether this value should be changed with the neighboring value or not.

Step 5: Terminating Criterion Controlling
Steps 2 through 4 are repeated until a termination criterion is fulfilled. Any terminating condition can be considered, and in this study the optimization process is terminated after a fixed number of iterations.

17.5 Search Behavior of the Vibrating Particles System Algorithm

In order to evaluate the effect of the algorithm parameters on the optimization results, a spatial 120-bar dome-shaped truss (Sect. 17.6.1) is considered as a benchmark. The effect of the population size, the maximum number of structural analyses (population size × total number of iterations), α, p, w_1, and w_2 are investigated in this section. In the first step, these parameters are set to 20, 20000, 0.15, 70 %, 0.3, and 0.3, respectively, and then their proper values are obtained one after another.

Tables 17.1 and 17.2 summarize the statistical results achieved for different values of population size (10, 20, 30, and 40) and total number of iterations (750, 1000, 1250, and 1500), respectively. As it can be seen from Table 17.1, when population size is

Table 17.1 Sensitivity analysis on population size

	10	20	30	40
Best optimized weight (lb)	33,262.75	33,250.27	33,255.65	33,471.79
Worst optimized weight (lb)	33,413.99	33,282.16	33,432.60	33,903.75
Average optimized weight (lb)	33,322.28	33,258.58	33,315.24	33,668.73
Standard deviation on average weight (lb)	51.49	10.31	62.77	130.71
Number of structural analyses for the best design	8920	19,780	13,060	9780
Average number of structural analysis	10,106	16,930	12,746	7958

Table 17.2 Sensitivity analysis on maximum number of iterations

	750	1000	1250	1500
Best optimized weight (lb)	33,251.34	33,250.27	33,250.83	33,250.24
Worst optimized weight (lb)	33,283.49	33,282.16	33,275.18	33,265.92
Average optimized weight (lb)	33,263.52	33,258.59	33,255.03	33,257.01
Standard deviation on average weight (lb)	12.75	10.31	7.71	5.97
Number of structural analyses for the best design	12,620	19,780	20,800	22,320
Average number of structural analysis	13,094	16,930	18,646	20,802

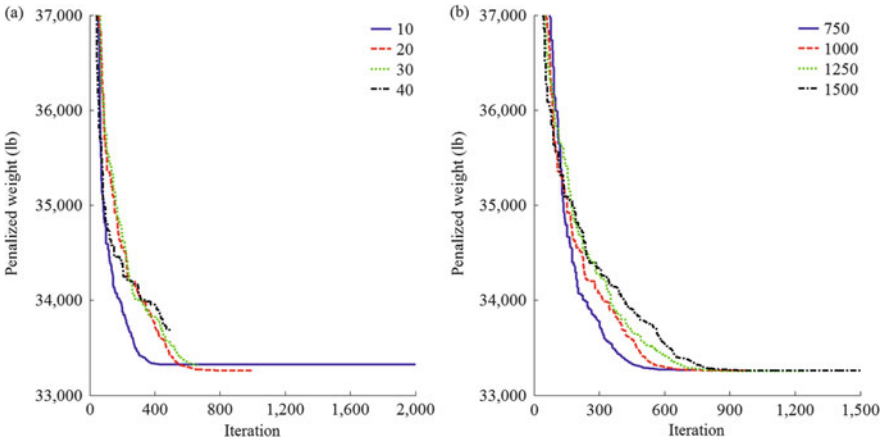

Fig. 17.6 Sensitivity analysis on (**a**) population size and (**b**) maximum number of iterations

20, the VPS has better performance in terms of the best weight, worst weight, average optimized weight, and standard deviation on average weight. Table 17.2 demonstrates that considering 1500 iterations is the most efficient value for the total number of iterations. The corresponding average convergence curves are shown in Fig. 17.6. Since the maximum number of structural analyses is set to 20,000 in Fig. 17.6a, the total number of iterations for 10, 20, 30, and 40 particles are 2000, 1000, 667, and 500, respectively, considered as the termination criterion.

Performance of the VPS with different values of α (0.05, 0.1, 0.15, and 0.2) and p (60 %, 70 %, 80 %, and 90 %) are compared in Tables 17.3 and 17.4, respectively. When α is considered as 0.1, the best weight is achieved; however, comparison of the other variables shows that 0.05 is generally the most suitable value for α. It can be concluded from Table 17.4 that 70 % is the most efficient value for p. Average convergence histories are depicted in Fig. 17.7. As mentioned before, the influence of damping level on vibration is similar to the effect of α on particles convergence as can be seen in Fig. 17.7a. To make the curves of Fig. 17.7b clearer, the magnified version of lower part is also shown.

Results of sensitivity analysis on w_1 and w_2 are shown in Tables 17.5 and 17.6. According to the statistical results reported in these tables, the most suitable

Table 17.3 Sensitivity analysis on α

	0.05	0.1	0.15	0.2
Best optimized weight (lb)	33,249.98	33,249.76	33,250.24	33,249.98
Worst optimized weight (lb)	33,262.74	33,283.46	33,265.92	33,261.82
Average optimized weight (lb)	33,253.56	33,254.91	33,257.01	33,254.02
Standard deviation on average weight (lb)	4.36	10.31	5.97	3.89
Number of structural analyses for the best design	8280	17,500	22,320	24,180
Average number of structural analyses	9846	17,794	20,802	24,834

Table 17.4 Sensitivity analysis on p

	60 %	70 %	80 %	90 %
Best optimized weight (lb)	33,250.06	33,249.98	33,250.89	33,250.08
Worst optimized weight (lb)	33,260.61	33,262.74	33,257.86	33,281.97
Average optimized weight (lb)	33,254.03	33,253.56	33,253.23	33,256.93
Standard deviation on average weight (lb)	4.27	4.36	2.54	9.75
Number of structural analyses for the best design	12,900	8280	10,580	10,740
Average number of structural analysis	11,114	9846	11,910	10,104

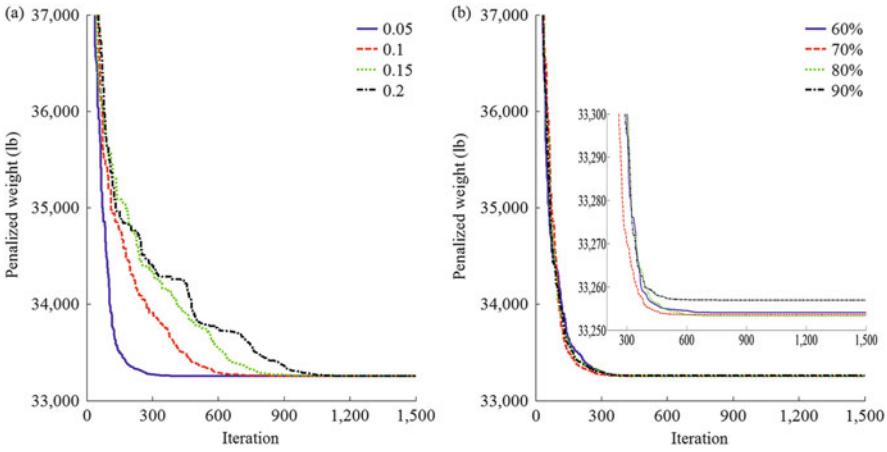

Fig. 17.7 Sensitivity analysis on (**a**) α and (**b**) p

performance of the VPS is obtained when the value of 0.3 is considered for w_1 and w_2. Figure 17.8 compares the average convergence curves. It can be seen from Fig. 17.8a that by decreasing the value of w_1 (decreasing the effect of *HB* position in updating formula), the exploration is increased and vice versa. In order to make the curves of Fig. 17.8b more clear, the magnified version of lower part is also added.

Table 17.5 Sensitivity analysis on w_1

	0.2	0.25	0.3	0.35
Best optimized weight (lb)	33,386.52	33,250.16	33,249.98	33,252.79
Worst optimized weight (lb)	33,655.38	33,268.67	33,262.74	33,676.11
Average optimized weight (lb)	33,484.02	33,254.51	33,253.56	33,314.71
Standard deviation on average weight (lb)	83.68	5.38	4.36	130.57
Number of structural analyses for the best design	28,820	28,540	8280	5160
Average number of structural analysis	26,456	28,342	9846	6520

Table 17.6 Sensitivity analysis on w_2

	0.2	0.25	0.3	0.35
Best optimized weight (lb)	33,250.63	33,249.67	33,249.98	33,250.62
Worst optimized weight (lb)	33,268.43	33,271.20	33,262.74	33,321.25
Average optimized weight (lb)	33,255.19	33,255.38	33,253.56	33,264.93
Standard deviation on average weight (lb)	5.06	6.49	4.36	22.84
Number of structural analyses for the best design	12,940	12,180	8280	12,880
Average number of structural analysis	11,982	12,196	9846	9954

In summary, the values of population size, the total number of iteration, α, p, w_1, and w_2 are set to 20, 1500, 0.05, 70 %, 0.3, and 0.3 for all examples, respectively.

17.6 Test Problems and Optimization Results

Four skeletal structures are optimized for minimum weight with the cross-sectional areas of the members being the design variables to evaluate the performance of the proposed method. The examples are classified into two groups: the first group consists of two truss structures with the number of truss bars of 120 and 200, respectively, and the second group includes two steel frames having 105 and 168 members, respectively. For all the considered examples, 20 independent optimization runs are carried out as metaheuristic algorithms have stochastic nature and their performance may be sensitive to initial population. The algorithm is coded in MATLAB, and the structures are analyzed using the direct stiffness method by our own codes.

17.6.1 A Spatial 120-Bar Dome-Shaped Truss

- The schematic and element grouping of the spatial 120-bar dome truss are shown in Fig. 17.9. The structure is divided into seven groups of elements because of

Table 17.7 Performance comparison for the spatial 120-bar dome-shaped truss structure

Element group	Optimal cross-sectional areas (in^2)						
	CSS (Kaveh and Talatahari [10])	IRO (Kaveh et al. [11])	MSPSO (Talatahari et al. [12])	CBO (Kaveh and Mahdavi [13])	TWO (Kaveh and Zolghadr [14])	WEO (Kaveh and Bakhshpoori [15])	Present work [1]
1	3.027	3.0252	3.0244	3.0273	3.0247	3.0243	3.0244
2	14.606	14.8354	14.7804	15.1724	14.7261	14.7943	14.7536
3	5.044	5.1139	5.0567	5.2342	5.1338	5.0618	5.0789
4	3.139	3.1305	3.1359	3.119	3.1369	3.1358	3.1371
5	8.543	8.4037	8.4830	8.1038	8.4545	8.4870	8.4829
6	3.367	3.3315	3.3104	3.4166	3.2946	3.2886	3.3012
7	2.497	2.4968	2.4977	2.4918	2.4956	2.4967	2.4963
Weight (lb)	33,251.9	33,256.48	33,251.22	33,286.3	33,250.31	33,250.24	33,249.98
Average optimized weight (lb)	N/A	33,280.85	33,257.29	33,398.5	33,282.64	33,255.55	33,253.56
Standard deviation on average weight (lb)	N/A	N/A	4.29	67.09	25.38	N/A	4.36
Number of structural analyses	7000	18,300	15,000	14,960	16,000	19,510	8280

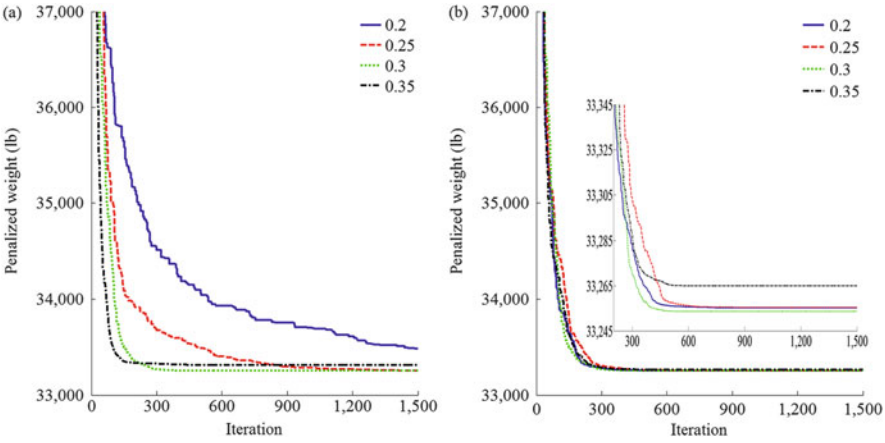

Fig. 17.8 Sensitivity analysis on (**a**) w_1 and (**b**) w_2

symmetry (for the sake of clarity, not all the element groups are numbered in Fig. 17.9). The modulus of elasticity is 30,450 ksi (210 GPa) and the material density is 0.288 lb/in^3 (7971.810 kg/m^3). The yield stress of steel is taken as 58.0 ksi (400 MPa). The dome is considered to be subjected to vertical loading at all unsupported joints. These loads are taken as −13.49 kips (−60 kN) at node 1, −6.744 kips (−30 kN) at nodes 2 through 14, and −2.248 kips (−10 kN) at the rest of the nodes. Element cross-sectional areas can vary between 0.775 in^2 (5 cm^2) and 20.0 in^2 (129.032 cm^2). Displacement limitations of ±0.1969 in (±5 mm) are imposed on all nodes in x-, y-, and z-coordinate directions. Constraints on member stresses are imposed according to the provisions of the AISC [9] as follows:

The allowable tensile stresses for tension members are calculated as:

$$\sigma_i^+ = 0.6F_y \tag{17.13}$$

where F_y is the yield strength.

The allowable stress limits for compression members are calculated depending on two possible failure modes of the members known as elastic and inelastic buckling. Therefore

$$\sigma_i^- = \begin{cases} \left[\left(1 - \dfrac{\lambda_i^2}{2C_c^2}\right)F_y\right] \Big/ \left[\dfrac{5}{3} + \dfrac{3\lambda_i}{8C_c} - \dfrac{\lambda_i^3}{8C_c^3}\right] & \text{for } \lambda_i < C_c \\ \dfrac{12\pi^2 E}{23\lambda_i^2} & \text{for } \lambda_i \geq C_c \end{cases} \tag{17.14}$$

where E is the modulus of elasticity; λ_i is the slenderness ratio ($\lambda_i = kl_i/r_i$); C_c denotes the slenderness ratio dividing the elastic and inelastic buckling regions

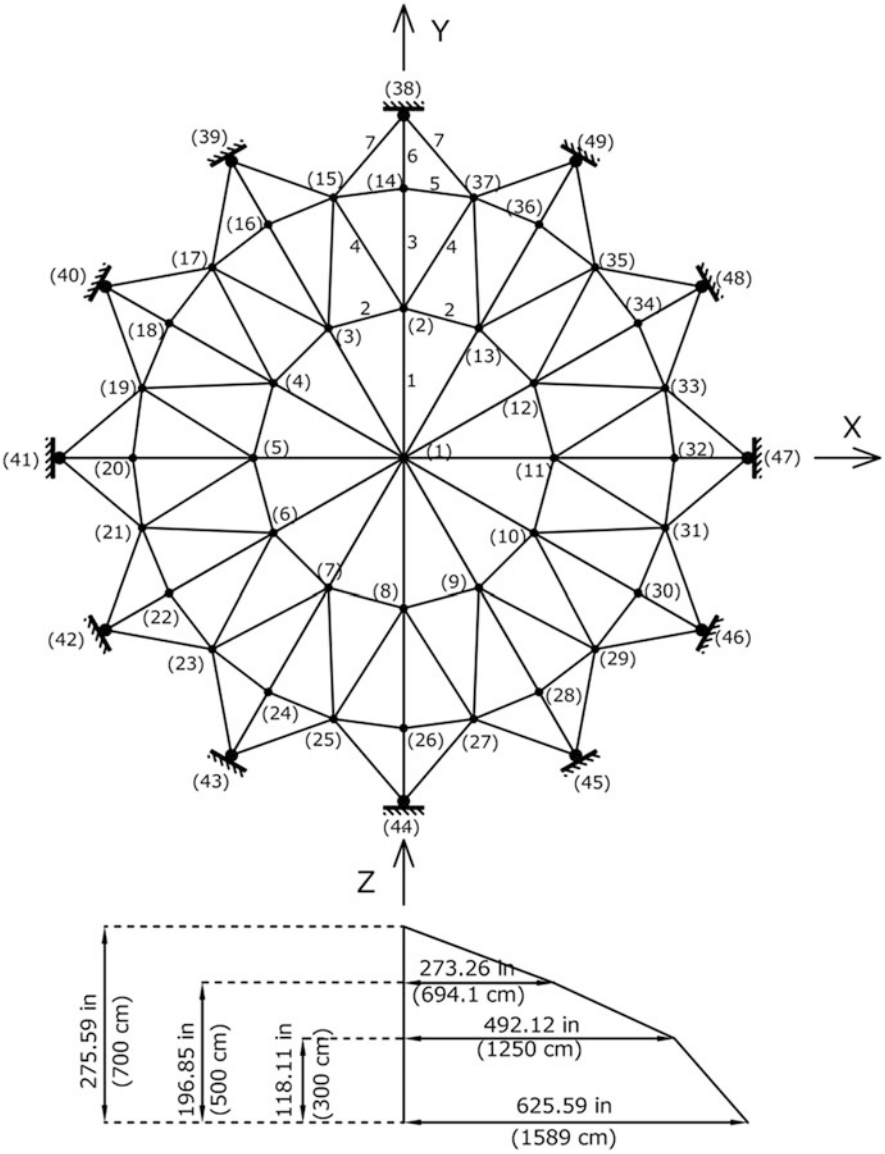

Fig. 17.9 Schematic of the spatial 120-bar dome-shaped truss

$C_c = \sqrt{2\pi^2 E / F_y}$; k is the effective length factor (k is set equal to 1 for all truss members); L_i is the member length; and r_i is the minimum radius of gyration.

This truss was previously optimized by CSS (charged system search algorithm) (Kaveh and Talatahari [10]), IRO (improved ray optimization) (Kaveh et al. [11]),

MSPSO (multi-stage particle swarm optimization) (Talatahari et al. [12]), CBO (colliding bodies optimization) (Kaveh and Mahdavi [13]), TWO (tug of war optimization) (Kaveh and Zolghadr [14]), and WEO (water evaporation optimization) (Kaveh and Bakhshpoori [15]).

Comparison of the optimal designs obtained by this work with those of the other researches is given in Table 17.7. It can be seen that the lightest design (i.e., 33,249.98 lb) and the best average optimized weight (i.e., 33,253.56 lb) are found by the proposed method. The VPS converges to the optimum solution after 8280 analyses. The CSS gives the best result as 33,251.9 lb in 7000 analyses. However, the VPS achieves this result after 6400 analyses. Figure 17.10 compares the convergence curves of the best and the average results obtained by the proposed method.

17.6.2 A 200-Bar Planar Truss

The second structural optimization problem solved in this chapter is the optimal design of the 200-bar planar truss schematized in Fig. 17.11. Due to the symmetry, the elements are divided into 29 groups. The modulus of elasticity and the material density of members are 210 GPa and 7860 kg/m^3, respectively. Nonstructural masses of 100 kg are attached to the upper nodes. A lower bound of 0.1 cm^2 is assumed for the cross-sectional areas. The first three natural frequencies of the structure must satisfy the following limitations ($f_1 \geq 5$ Hz, $f_2 \geq 10$ Hz, $f_3 \geq 15$ Hz).

Table 17.8 presents the results of the optimal designs utilizing CSS–BBBC (a hybridization of the charged system search and the Big Bang–Big Crunch algorithms with trap recognition capability) (Kaveh and Zolghadr [16]), CBO

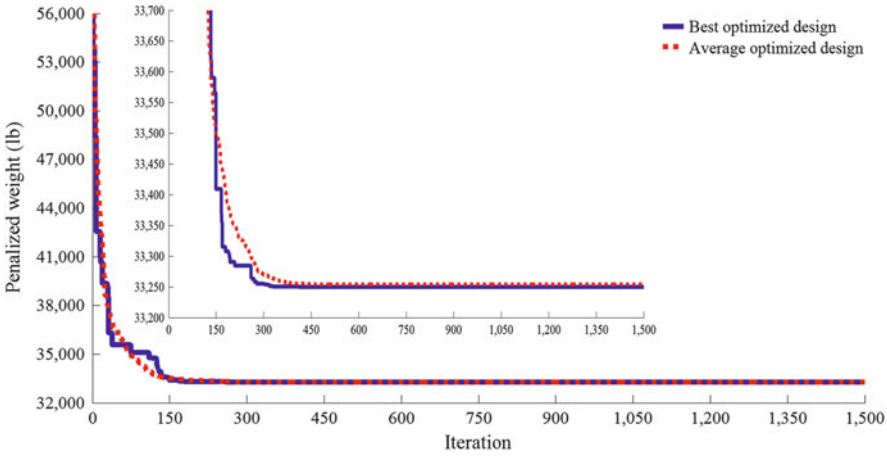

Fig. 17.10 Convergence curves obtained for the 120-bar dome-shaped truss problem

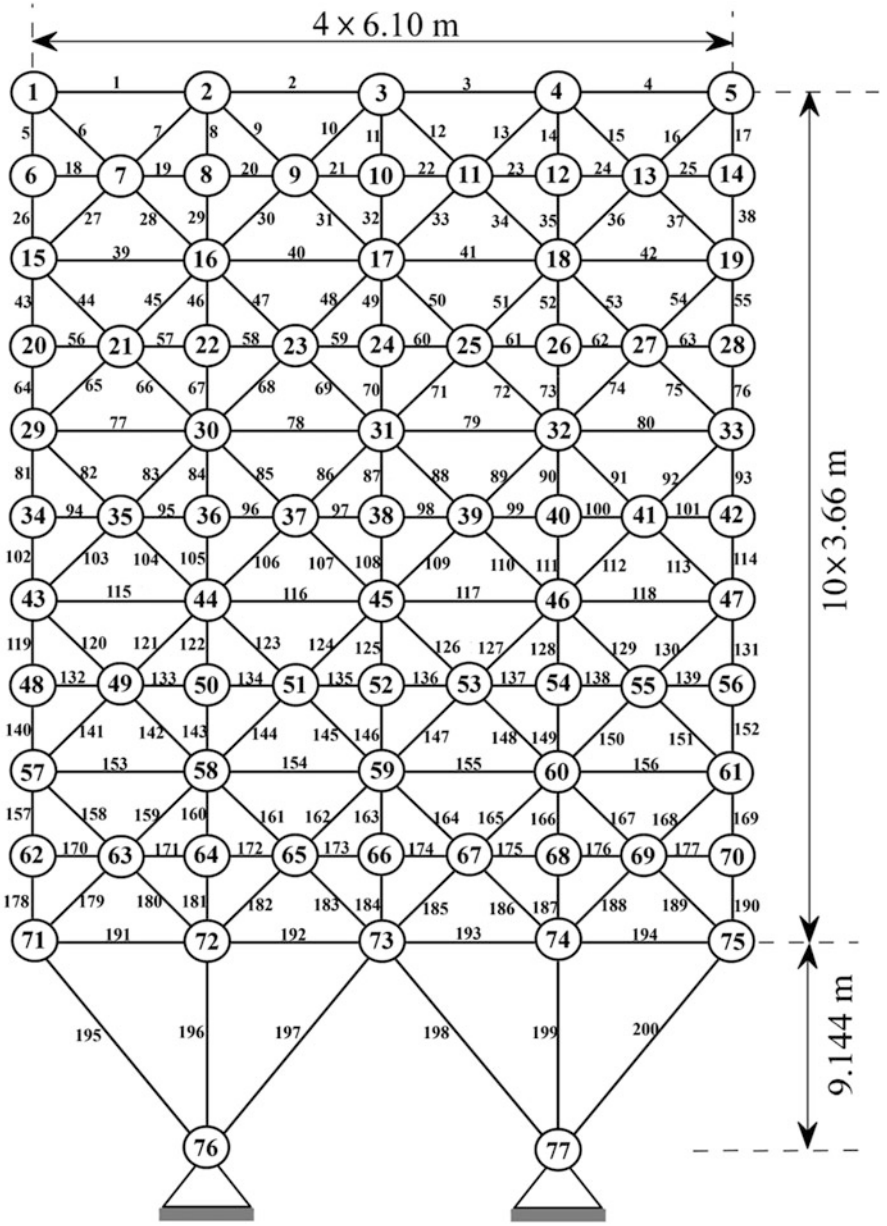

Fig. 17.11 Schematic of the 200-bar planar truss

(colliding bodies optimization) (Kaveh and Ilchi Ghazaan [17]), ECBO (enhanced colliding bodies optimization) (Kaveh and Ilchi Ghazaan [17]), CBO–PSO (a hybrid of CBO and PSO algorithms) (Kaveh and Mahdavi [18]), and the

Table 17.8 Performance comparison for the 200-bar planar truss structure

Element group	Members in the group	Areas (cm^2)				
		CSS–BBBC (Kaveh and Zolghadr [28])	CBO (Kaveh and Ilchi Ghazaan [29])	ECBO (Kaveh and Ilchi Ghazaan [29])	CBO–PSO (Kaveh and Mahdavi [30])	Present work [1]
1	1, 2, 3, 4	0.2934	0.3059	0.2993	0.2797	0.3031
2	5, 8, 11, 14, 17	0.5561	0.4476	0.4497	0.6968	0.4496
3	19, 20, 21, 22, 23, 24	0.2952	0.1000	0.1000	0.1000	0.1002
4	18, 25, 56, 63, 94, 101, 132, 139, 170, 177	0.1970	0.1001	0.1000	0.1000	0.1000
5	26, 29, 32, 35, 38	0.8340	0.4944	0.5137	0.5796	0.5086
6	6, 7, 9, 10, 12, 13, 15, 16, 27, 28, 30, 31, 33, 34, 36, 37	0.6455	0.8369	0.7914	0.8213	0.8204
7	39, 40, 41, 42	0.1770	0.1001	0.1013	0.1279	0.1000
8	43, 46, 49, 52, 55	1.4796	1.5514	1.4129	1.0152	1.4210
9	57, 58, 59, 60, 61, 62	0.4497	0.1000	0.1019	0.1000	0.1002
10	64, 67, 70, 73, 76	1.4556	1.5286	1.6460	1.5647	1.5900
11	44, 45, 47, 48, 50, 51, 53, 54, 65, 66, 68, 69, 71, 72, 74, 75	1.2238	1.1547	1.1532	1.6465	1.1530
12	77, 78, 79, 80	0.2739	0.1000	0.1000	0.2296	0.1277
13	81, 84, 87, 90, 93	1.9174	2.9980	3.1850	2.9007	2.9160
14	95, 96, 97, 98, 99, 100	0.1170	0.1017	0.1034	0.1000	0.1009
15	102, 105, 108, 111, 114	3.5535	3.2475	3.3126	3.0133	3.2826
16	82, 83, 85, 86, 88, 89, 91, 92, 103, 104, 106, 107, 109, 110, 112, 113	1.3360	1.5213	1.5920	1.6142	1.5856
17	115, 116, 117, 118	0.6289	0.3996	0.2238	0.2755	0.2794
18	119, 122, 125, 128, 131	4.8335	4.7557	5.1227	5.0951	5.0680
19	133,134,135,136,137,138	0.6062	0.1002	0.1050	0.1000	0.1004

20	140,143,146,149,152	5.4393	5.1359	5.3707	5.5172	5.4760
21	120, 121, 123, 124, 126, 127, 129, 130, 141, 142, 144, 145, 147, 148, 150, 151	1.8435	2.1181	2.0645	2.2032	2.1169
22	153, 154, 155, 156	0.8955	0.9200	0.5443	0.8659	0.6939
23	157, 160, 163, 166, 169	8.1759	7.3084	7.6497	7.6477	7.6912
24	171, 172, 173, 174, 175, 176	0.3209	0.1185	0.1000	0.1000	0.1332
25	178, 181, 184, 187, 190	10.98	7.6901	7.6754	8.1273	7.9972
26	158, 159, 161, 162, 164, 165, 167, 168, 179, 180, 182, 183, 185, 186, 188, 189	2.9489	3.0895	2.7178	2.9665	2.7859
27	191, 192, 193, 194	10.5243	10.6462	10.8141	10.2386	10.4331
28	195, 197, 198, 200	20.4271	20.7190	21.6349	20.6364	21.2289
29	196, 199	19.0983	11.7463	10.3520	11.6468	10.7392
Weight (kg)		2298.61	2161.15	2158.08	2195.469	2156.62
Average optimized weight (kg)		N/A	2447.52	2159.93	N/A	2159.46
Standard deviation on average weight (kg)		N/A	301.29	1.57	N/A	2.79
Number of structural analyses		N/A	10,500	14,700	9000	16,420

proposed method. The weight of the best result obtained by VPS is 2156.62 kg that is the best among the compared methods. Moreover, the average optimized weight for 20 independent optimization runs of the VPS is 2159.46 kg which is less than those of all other methods. The first three natural frequencies of the structure for the best design are 5.0000 Hz, 12.2086 Hz, and 15.0153 Hz. The proposed method requires 16,420 structural analyses to find the optimum solution, while CBO, ECBO, and CBO–PSO require 10,500, 14,700, and 9000 structural analyses, respectively. It should be noted that the designs found by VPS at 9000th, 10,500th, and 14,700th analyses are 2158.35 kg, 2158.06 kg, and 2157.72 kg, respectively. Comparison of the convergence rates between the best and the average curves of VPS is illustrated in Fig. 17.12.

17.6.3 A 3-Bay 15-Story Frame Structure

Figure 17.13 represents the schematic of the 3-bay 15-story frame. The applied loads and the numbering of member groups are also shown in this figure. The modulus of elasticity is 29 Msi (200 GPa) and the yield stress is 36 ksi (248.2 MPa). The effective length factors of the members are calculated as $k_x \geq 0$ for a sway-permitted frame, and the out-of-plane effective length factor is specified as $k_y = 1.0$. Each column is considered as non-braced along its length, and the non-braced length for each beam member is specified as one-fifth of the span length. Limitation on displacement and strength are imposed according to the provisions of the AISC [19] as follows:

(a) Maximum lateral displacement

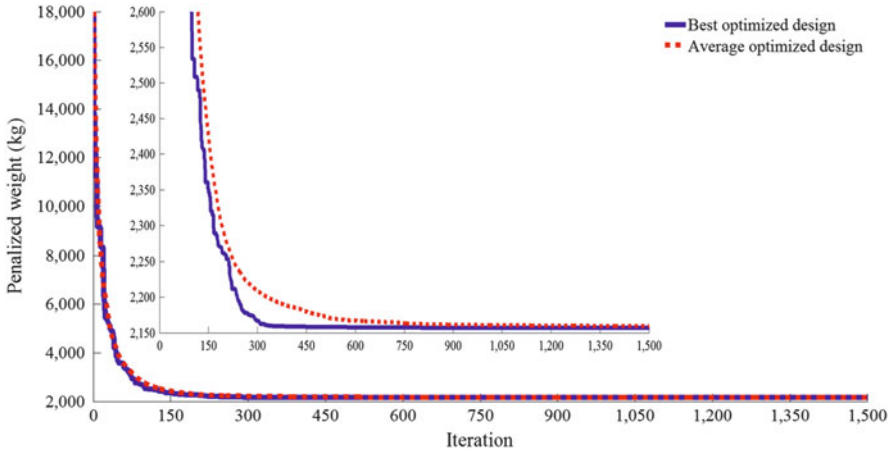

Fig. 17.12 Convergence curves obtained for the 200-bar planar truss problem

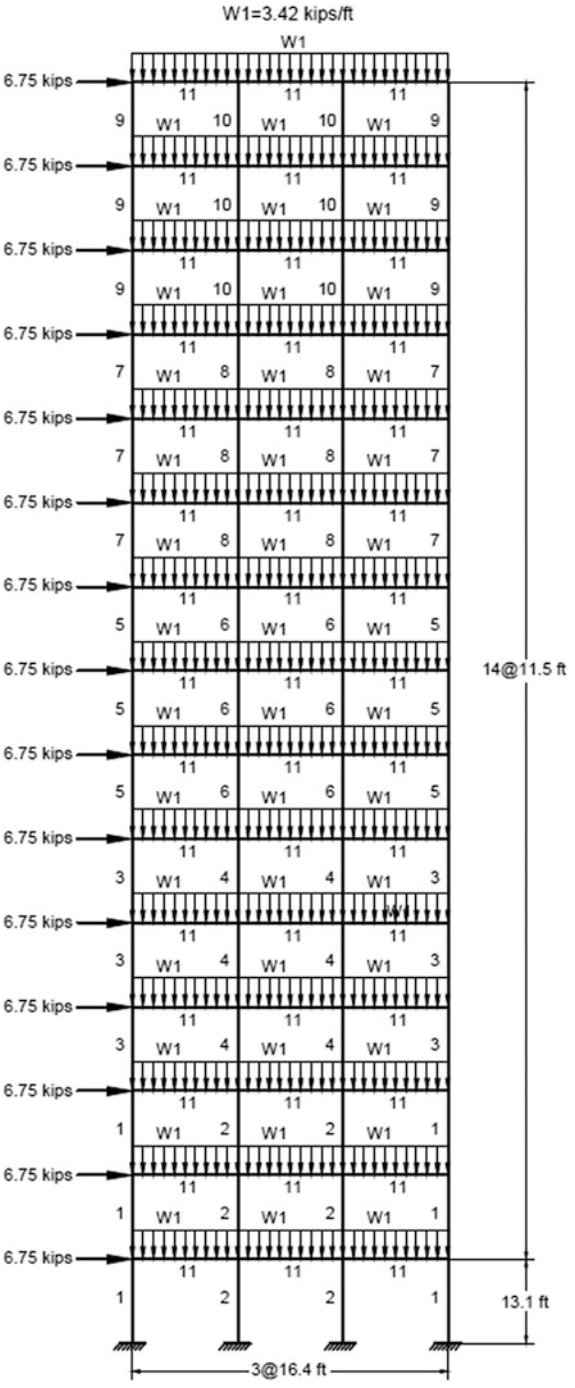

Fig. 17.13 Schematic of the 3-bay 15-story frame

$$\frac{\Delta_T}{H} - R \leq 0 \tag{17.15}$$

where Δ_T is the maximum lateral displacement; H is the height of the frame structure; and R is the maximum drift index which is equal to 1/300.

(b) The inter-story displacements

$$\frac{d_i}{h_i} - R_I \leq 0, \quad i = 1, 2, \ldots, ns \tag{17.16}$$

where d_i is the inter-story drift; h_i is the story height of the ith floor; ns is the total number of stories; and R_I is the inter-story drift index (1/300).

(c) Strength constraints

$$\begin{cases} \dfrac{Pu}{2\varphi_c P_n} + \dfrac{M_u}{\varphi_b M_n} - 1 \leq 0, & for \dfrac{Pu}{\varphi_c P_n} < 0.2 \\ \dfrac{Pu}{\varphi_c P_n} + \dfrac{8M_u}{9\varphi_b M_n} - 1 \leq 0, & for \dfrac{Pu}{\varphi_c P_n} \geq 0.2 \end{cases} \tag{17.17}$$

where P_u is the required axial strength (tension or compression); P_n is the nominal axial strength (tension or compression); φ_c is the resistance factor ($\varphi_c = 0.9$ for tension, $\varphi_c = 0.85$ for compression); M_u is the required flexural strengths; M_n is the nominal flexural strengths; and φ_b denotes the flexural resistance reduction factor ($\varphi_b = 0.90$).

The nominal tensile strength for yielding in the gross section is calculated by:

$$P_n = A_g . F_y \tag{17.18}$$

The nominal compressive strength of a member is computed as:

$$P_n = A_g . F_{cr} \tag{17.19}$$

where

$$\begin{cases} F_{cr} = \left(0.658\ \lambda_c^2\right) F_y, & for\ \ \lambda_c \leq 1.5 \\ F_{cr} = \left(\dfrac{0.877}{\lambda_c^2}\right) F_y, & for\ \ \lambda_c > 1.5 \end{cases} \tag{17.20}$$

$$\lambda_c = \frac{kl}{r\pi}\sqrt{\frac{F_y}{E}} \tag{17.21}$$

where A_g is the cross-sectional area of a member and k is the effective length factor that is calculated by (Dumonteil [20]):

$$k = \sqrt{\frac{1.6G_AG_B + 4.0(G_A + G_B) + 7.5}{G_A + G_B + 7.5}} \tag{17.22}$$

where G_A and G_B are stiffness ratios of columns and girders at the two end joints, A and B, of the column section, respectively.

Also, in this example the sway of the top story is limited to 9.25 in (23.5 cm).

Table 17.9 presents the comparison of the results of the present algorithm with the outcomes of other algorithms. The proposed method yields the least weight for this example, which is 86,985 lb. The other design weights are 95,850 lb by HPSACO (a hybrid algorithm of harmony search, particle swarm and ant colony) (Kaveh and Talatahari [21]), 97,689 lb by HBB–BC (a hybrid Big Bang–Big Crunch optimization) (Kaveh and Talatahari [22]), 93,846 lb by ICA (imperialist competitive algorithm) (Kaveh and Talatahari [23]), 92,723 lb by CSS (Kaveh and Talatahari [24]), 93,795 lb by CBO (Kaveh and Ilchi Ghazaan [25]), 86,986 lb by ECBO (Kaveh and Ilchi Ghazaan [25]), and 93,315 lb by ES–DE (eagle strategy with differential evolution) (Talatahari et al. [26]). The best design of VPS has been achieved in 19,600 analyses. It should be noted that the proposed method achieved about 92,000 lb (the best weight among the other methods except ECBO) after 10,800 structural analyses. Figure 17.14 provides the convergence rates of the best and average results found by the VPS. Element stress ratio and inter-story drift evaluated at the best design optimized by VPS are shown in Fig. 17.15. The maximum stress ratio is 99.88 % and the maximum inter-story drift is 45.41.

17.6.4 A 3-Bay 24-Story Frame Structure

The last structural optimization problem solved in this chapter is the weight minimization of the 3-bay 24-story frame schematized in Fig. 17.16. Frame members are collected in 20 groups (16 column groups and 4 beam groups). Each of the four beam element groups is chosen from all 267 W-shapes, while the 16 column element groups are limited to W14 sections. The material has a modulus of elasticity equal to $E = 29.732$ Msi (205 GPa) and a yield stress of $f_y = 33.4$ ksi (230.3 MPa). The effective length factors of the members are calculated as $k_x \geq 0$ for a sway-permitted frame, and the out-of-plane effective length factor is specified as $k_y = 1.0$. All columns and beams are considered as non-braced along their lengths. Similar to the previous example, the frame is designed following the LRFD–AISC specification and uses an inter-story drift displacement constraint (AISC [19]).

This steel frame structure was previously optimized by ACO (ant colony optimization) (Camp et al. [27]), HS (harmony search) (Degertekin [28]), ICA (Kaveh and Talatahari [23]), CSS (Kaveh and Talatahari [24]), CBO (Kaveh and Ilchi Ghazaan [25]), ECBO (Kaveh and Ilchi Ghazaan [25]), and ES–DE (Talatahari et al. [26]). Table 17.10 presents a comparison between the results of the optimal

Table 17.9 Performance comparison for the 3-bay 15-story frame structure

Element group	Optimal W-shaped sections							
	HPSACO (Kaveh and Talatahari [21])	HBB–BC (Kaveh and Talatahari [22])	ICA (Kaveh and Talatahari [23])	CSS (Kaveh and Talatahari [24])	CBO (Kaveh and Ilchi Ghazaan [25])	ECBO (Kaveh and Ilchi Ghazaan [25])	ES–DE (Talatahari et al. [26])	Present work [1]
1	W21 × 111	W24 × 117	W24 × 117	W21 × 147	W24 × 104	W14 × 99	W18 × 106	W14 × 90
2	W18 × 158	W21 × 132	W21 × 147	W18 × 143	W40 × 167	W27 × 161	W36 × 150	W36 × 170
3	W10 × 88	W12 × 95	W27 × 84	W12 × 87	W27 × 84	W27 × 84	W12 × 79	W14 × 82
4	W30 × 116	W18 × 119	W27 × 114	W30 × 108	W27 × 114	W24 × 104	W27 × 114	W24 × 104
5	W21 × 83	W21 × 93	W14 × 74	W18 × 76	W21 × 68	W14 × 61	W30 × 90	W21 × 68
6	W24 × 103	W18 × 97	W18 × 86	W24 × 103	W30 × 90	W30 × 90	W10 × 88	W18 × 86
7	W21 × 55	W18 × 76	W12 × 96	W21 × 68	W8 × 48	W14 × 48	W18 × 71	W21 × 48
8	W27 × 114	W18 × 65	W24 × 68	W14 × 61	W21 × 68	W14 × 61	W18 × 65	W14 × 61
9	W10 × 33	W18 × 60	W10 × 39	W18 × 35	W14 × 34	W14 × 30	W8 × 28	W12 × 30
10	W18 × 46	W10 × 39	W12 × 40	W10 × 33	W8 × 35	W12 × 40	W12 × 40	W10 × 39
11	W21 × 44	W21 × 48	W21 × 44	W21 × 44	W21 × 50	W21 × 44	W21 × 48	W21 × 44
Weight (lb)	95,850	97,689	93,846	92,723	93,795	86,986	93,315	86,985
Average optimized weight (lb)	N/A	N/A	N/A	N/A	98,738	88,410	98,531	90,066
Standard deviation on average weight (lb)	N/A	N/A	N/A	N/A	N/A	N/A	3294	2533
Number of structural analyses	6800	9900	6000	5000	9520	9000	10,000	19,600

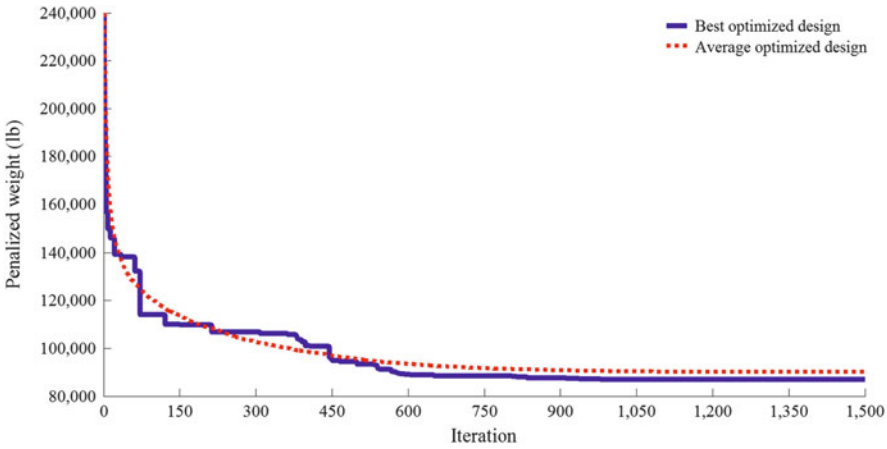

Fig. 17.14 Convergence curves obtained for the 3-bay 15-story frame structure

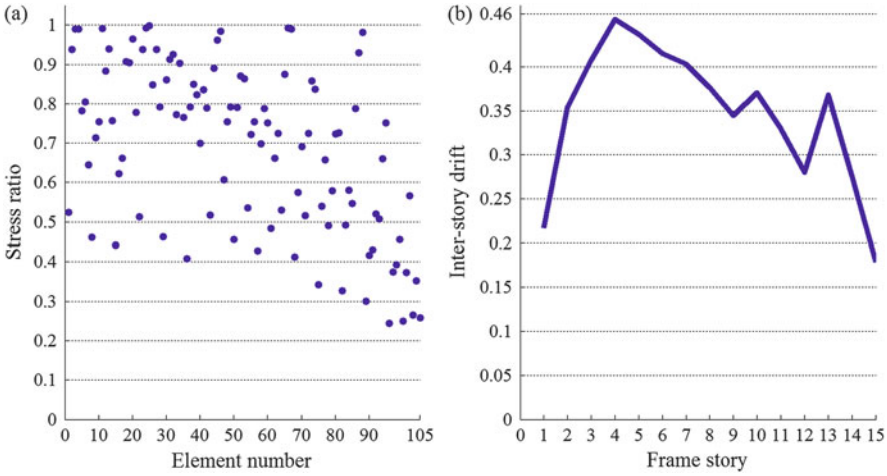

Fig. 17.15 Constraint margins for the best design obtained by VPS for the 3-bay 15-story frame problem: (**a**) element stress ratio and (**b**) inter-story drift

designs reported in the literature and the present work [1]. The lightest design (i.e., 201,618 lb) is found by ECBO algorithm and after that the best design belongs to VPS (i.e., 202,998 lb). The best design has been achieved at 16,220 analyses for VPS, and it obtained 209,532 lb after 8800 analyses, which is the best result compared to the weight achieved by the other methods. Figure 17.17 provides the convergence rates of the best and average results found by the proposed method.

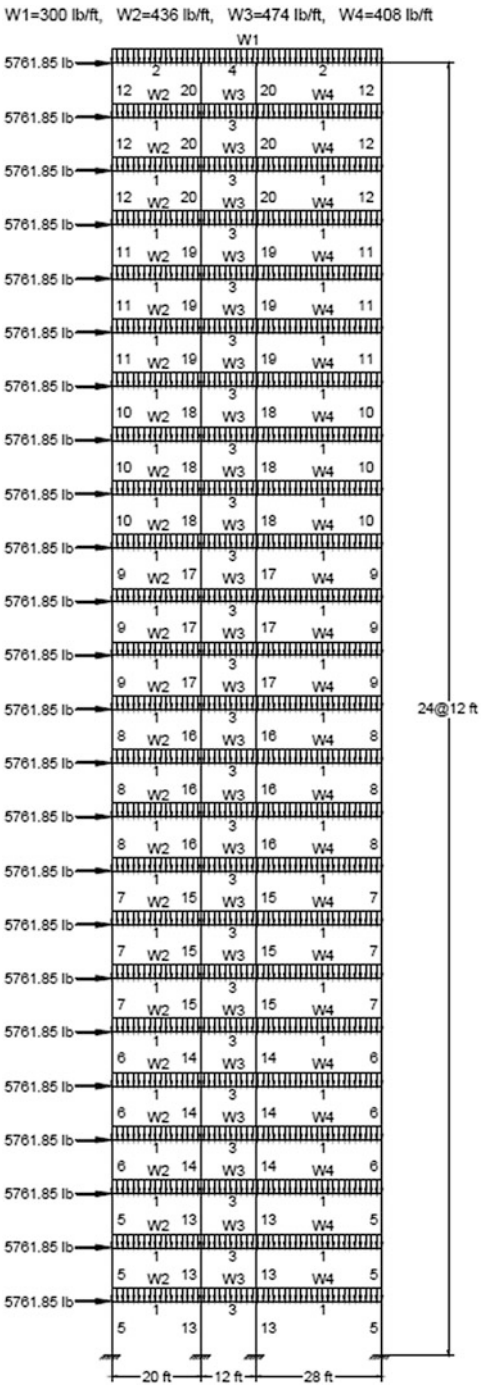

Fig. 17.16 Schematic of the 3-bay 24-story frame

Table 17.10 Performance comparison for the 3-bay 24-story frame structure

Element group	Optimal W-shaped sections							
	ACO (Camp et al. [27])	HS (Degertekin [28])	ICA (Kaveh and Talatahari [23])	CSS (Kaveh and Talatahari [24])	CBO (Kaveh and Ilchi Ghazaan [25])	ECBO (Kaveh and Ilchi Ghazaan [25])	ES–DE (Talatahari et al. [26])	Present work [1]
1	W30 × 90	W30 × 90	W30 × 90	W30 × 90	W27 × 102	W30 × 90	W30 × 90	W30 × 90
2	W8 × 18	W10 × 22	W21 × 50	W21 × 50	W8 × 18	W6 × 15	W21 × 55	W8 × 18
3	W24 × 55	W18 × 40	W24 × 55	W21 × 48	W24 × 55	W24 × 55	W21 × 48	W21 × 48
4	W8 × 21	W12 × 16	W8 × 28	W12 × 19	W6 × 8.5	W6 × 8.5	W10 × 45	W6 × 8.5
5	W14 × 145	W14 × 176	W14 × 109	W14 × 176	W14 × 132	W14 × 145	W14 × 145	W14 × 176
6	W14 × 132	W14 × 176	W14 × 159	W14 × 145	W14 × 120	W14 × 132	W14 × 109	W14 × 145
7	W14 × 132	W14 × 132	W14 × 120	W14 × 109	W14 × 145	W14 × 99	W14 × 99	W14 × 99
8	W14 × 132	W14 × 109	W14 × 90	W14 × 90	W14 × 82	W14 × 90	W14 × 145	W14 × 82
9	W14 × 68	W14 × 82	W14 × 74	W14 × 74	W14 × 61	W14 × 74	W14 × 109	W14 × 82
10	W14 × 53	W14 × 74	W14 × 68	W14 × 61	W14 × 43	W14 × 38	W14 × 48	W14 × 38
11	W14 × 43	W14 × 34	W14 × 30	W14 × 34	W14 × 38	W14 × 38	W14 × 38	W14 × 30
12	W14 × 43	W14 × 22	W14 × 38	W14 × 34	W14 × 22	W14 × 22	W14 × 30	W14 × 30
13	W14 × 145	W14 × 145	W14 × 159	W14 × 145	W14 × 99	W14 × 99	W14 × 99	W14 × 90
14	W14 × 145	W14 × 132	W14 × 132	W14 × 132	W14 × 109	W14 × 99	W14 × 132	W14 × 99
15	W14 × 120	W14 × 109	W14 × 99	W14 × 109	W14 × 82	W14 × 99	W14 × 109	W14 × 99
16	W14 × 90	W14 × 82	W14 × 82	W14 × 82	W14 × 90	W14 × 82	W14 × 68	W14 × 90
17	W14 × 90	W14 × 61	W14 × 68	W14 × 68	W14 × 74	W14 × 68	W14 × 68	W14 × 61
18	W14 × 61	W14 × 48	W14 × 48	W14 × 43	W14 × 61	W14 × 61	W14 × 68	W14 × 61
19	W14 × 30	W14 × 30	W14 × 34	W14 × 34	W14 × 30	W14 × 30	W14 × 61	W14 × 34
20	W14 × 26	W14 × 22	W14 × 22	W14 × 22	W14 × 22	W14 × 22	W14 × 22	W14 × 26
Weight (lb)	220,465	214,860	212,640	212,364	215,874	201,618	212,492	202,998
Average optimized weight (lb)	229,555	222,620	N/A	215,226	225,071	209,644	N/A	212,289

(continued)

Table 17.10 (continued)

Element group	Optimal W-shaped sections							
	ACO (Camp et al. [27])	HS (Degertekin [28])	ICA (Kaveh and Talatahari [23])	CSS (Kaveh and Talatahari [24])	CBO (Kaveh and Ilchi Ghazaan [25])	ECBO (Kaveh and Ilchi Ghazaan [25])	ES–DE (Talatahari et al. [26])	Present work [1]
Standard deviation on average weight (lb)	4561	N/A	N/A	2448	N/A	N/A	N/A	8292
Number of structural analyses	15,500	13,924	7500	5500	8280	15,360	12,500	16,220

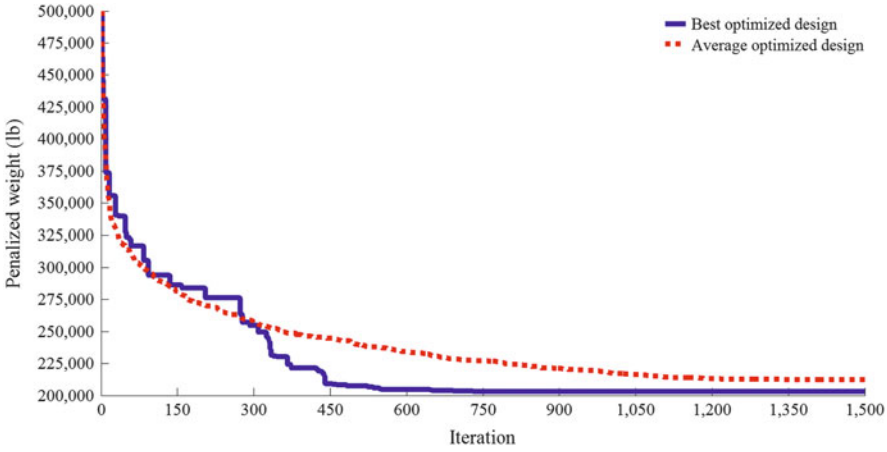

Fig. 17.17 Convergence curves obtained for the 3-bay 24-story frame problem

17.7 Concluding Remarks

This chapter presents a new population-based metaheuristic algorithm called vibrating particles system (VPS). This method is inspired by the damped free vibration of a single degree of freedom system. In the optimization process, particles gradually approach to their equilibrium positions. To maintain the balance between local search and global search, these equilibrium positions are obtained from the current population and the historically best position. Two truss and two frame benchmark structures are studied in order to show the performance of the VPS in terms of diversification, intensification, local optima avoidance, and convergence speed. The proposed algorithm finds superior optimal designs for three of the four problems investigated, illustrating the capability of the present method in solving constrained problems. Moreover, the average optimized results and standard deviation average results obtained by VPS are competitive with the other optimization methods. The convergence speed comparisons also reveal the fast-converging feature of the presented algorithm. For future research, it would be interesting to apply VPS to other optimization problems in different fields of science and engineering.

References

1. Kaveh A, Ilchi Ghazaan M (2016) A new meta-heuristic algorithm: vibrating particles system. Scientia Iranica, in press
2. Saka MP (1990) Optimum design of pin-joined steel structures with practical application. J Struct Eng 116:2599–2620
3. Erbatur F, Hasançebi O, Tütüncü I, Kiliç H (2000) Optimal design of planar and space structures with genetic algorithms. Comput Struct 75:209–224

4. Lee KS, Geem ZW (2004) A new structural optimization method based on the harmony search algorithm. Comput Struct 82:781–798
5. Hasançebi O, Çarbas S, Dogan E, Erdal F, Saka MP (2009) Performance evaluation of meta-heuristic search techniques in the optimum design of real size pin jointed structures. Comput Struct 87(5–6):284–302
6. Kazemzadeh Azad S, Hasançebi O (2015) Computationally efficient discrete sizing of steel frames via guided stochastic search heuristic. Comput Struct 156:12–28
7. Beer FP, Johnston ER Jr, Mazurek DF, Cornwell P, Self BP (2013) Vector mechanics for engineers. McGraw-Hill, New York, NY
8. Kaveh A, Talatahari S (2009) Particle swarm optimizer, ant colony strategy and harmony search scheme hybridized for optimization of truss structures. Comput Struct 87(5):267–283
9. American Institute of Steel Construction (AISC) (1989) Manual of steel construction: allowable stress design. American Institute of Steel Construction, Chicago, IL
10. Kaveh A, Talatahari S (2010) Optimal design of skeletal structures via the charged system search algorithm. Struct Multidiscip Optim 41:893–911
11. Kaveh A, Ilchi Ghazaan M, Bakhshpoori T (2013) An improved ray optimization algorithm for design of truss structures. Period Polytech-Civ Eng 57(2):97–112
12. Talatahari S, Kheirollahi M, Farahmandpour C, Gandomi AH (2013) A multi-stage particle swarm for optimum design of truss structures. Neural Comput Appl 23:1297–1309
13. Kaveh A, Mahdavi VR (2014) Colliding bodies optimization: a novel meta-heuristic method. Comput Struct 139:18–27
14. Kaveh A, Zolghadr A (2016) A novel meta-heuristic algorithm: tug of war optimization. Int J Optim Civil Eng 6(4):469–492
15. Kaveh A, Bakhshpoori T (2016) Water evaporation optimization: a novel physically inspired optimization algorithm. Comput Struct 167:69–85
16. Kaveh A, Zolghadr A (2012) Truss optimization with natural frequency constraints using a hybridized CSS–BBBC algorithm with trap recognition capability. Comput Struct 102–103:14–27
17. Kaveh A, Ilchi Ghazaan M (2014) Enhanced colliding bodies algorithm for truss optimization with frequency constraints. J Comput Civil Eng 29(6). 10.1061/(ASCE) CP.1943-5487.0000445, 04014104
18. Kaveh A, Mahdavi VR (2015) A hybrid CBO–PSO algorithm for optimal design of truss structures with dynamic constraints. Appl Soft Comput 34:260–273
19. American Institute of Steel Construction (AISC) (2001) Manual of steel construction: load and resistance factor design. American Institute of Steel Construction, Chicago, IL
20. Dumonteil P (1992) Simple equations for effective length factors. Eng J AISC 29(3):111–115
21. Kaveh A, Talatahari S (2009) Hybrid algorithm of harmony search, particle swarm and ant colony for structural design optimization. Stud Comput Int 239:159–198
22. Kaveh A, Talatahari S (2010) A discrete Big Bang–Big Crunch algorithm for optimal design of skeletal structures. Asian J Civil Eng 11(1):103–122
23. Kaveh A, Talatahari S (2010) Optimum design of skeletal structure using imperialist competitive algorithm. Comput Struct 88:1220–1229
24. Kaveh A, Talatahari S (2012) Charged system search for optimal design of frame structures. Appl Soft Comput 12:382–393
25. Kaveh A, Ilchi Ghazaan M (2015) A comparative study of CBO and ECBO for optimal design of skeletal structures. Comput Struct 153:137–147
26. Talatahari S, Gandomi AH, Yang XS, Deb S (2015) Optimum design of frame structures using the eagle strategy with differential evolution. Eng Struct 91:16–25
27. Camp CV, Bichon BJ, Stovall S (2005) Design of steel frames using ant colony optimization. J Struct Eng 131:369–379
28. Degertekin SO (2008) Optimum design of steel frames using harmony search algorithm. Struct Multidiscip Optim 36:393–401

29. Kaveh A, Ilchi Ghazaan M (2014) Enhanced colliding bodies algorithm for truss optimization with frequency constraints. J Comput Civil Eng 29(6)
30. Kaveh A, Mahdavi VR (2015) A hybrid CBO–PSO algorithm for optimal design of truss structures with dynamic constraints. Appl Soft Comput 34:260–273. doi:10.1061/(ASCE)CP.1943-5487.0000445,04014104